From Mono- to Polynuclear Coordination Complexes with a 2,2'-Bipyrimidine-4,4'-dicarboxylate Ligand

Piotr W Zabierowski, Olivier Jeannin, Thomas Fix, Jean-François Guillemoles, Loïc J Charbonnière, Aline M Nonat

From mono- to polynuclear coordination complexes with 2,2'-bipyrimidine-4,4'-dicarboxylate ligand

Piotr Zabierowski,[*,a,b,c] Olivier Jeannin,[d] Thomas Fix,[c] Jean-François Guillemoles,[a] Loïc J. Charbonnière,[b] and Aline M. Nonat[*,b]

[a] *Institut Photovoltaïque d'Ile-de-France 18, boulevard Thomas Gobert, 91120 Palaiseau, France*

[b] *Equipe de Synthèse pour l'Analyse, IPHC, UMR 7178 CNRS, Université de Strasbourg, ECPM, 25 rue Becquerel, 67087 Strasbourg Cedex, France*

[c] *Laboratoire ICube, 23 rue du Loess, BP20 CR F-67037, Strasbourg, Cedex 2 France*

[d] *Institut des Sciences Chimiques de Rennes, UMR-CNRS 6226, 263 Avenue du Général Leclerc, CS 74205, F-35042 Rennes Cedex, France*

E-mail: piotr.zabierowski@outlook.com; aline.nonat@unistra.fr

Abstract. The coordination properties of the ligand 2,2'-bipyrimidine-4,4'-dicarboxylic acid (H_2*bpd*) with lanthanide(III) ions (Ln = Eu, Tb, Lu) were investigated. The synthesis of the H_2*bpd* ligand and its salts ([K_2(*bpd*)(H_2O)$_2$] (1) and [(*Alk*NH)Lu(*bpd*)$_2$] (*Alk* = Et, Hex, en) are described. In the presence of $LnCl_3$ salts (Ln = Lu, Eu, Tb), the formation of [Ln(*bpd*)$_2$]$^-$ and [Ln(*bpd*)(H_2O)$_x$)]$^+$ species was assessed by ^{1}H NMR, spectrophotometry and spectrofluorometric

titrations in aqueous solution. The solid state structure of (1), $[K(H_2O)_2][Lu(bpd)_2]$ (2) and $[(Et_3NH)Lu(bpd)_2]$ (3) could be determined by X-ray diffraction, showing the ligand to act as a tetradentate unit with formation of three five membered chelate rings around the central Ln(III). With the aim of building polynuclear assemblies, the coordination between $[Lu(bdp)_2]^-$ and $[Lu(tta)_3(H_2O)]$ units (tta = thenoyltrifluoroacetylacetonate) was also investigated. In methanol, ^{1}H NMR titration experiments revealed the formation of complex mixtures from which two new species could be identified, $[Lu_2(bpd)(tta)_4]$ (4) and $H[Lu(bpd)(tta)_2]$ (5), as confirmed by their solid state structure analysis. Using highly lipophilic cations in chloroform, the octametallic complex $[enH]_4[Lu_8(bpd)_4(tta)_{18}]$ (6) could be isolated and its X-ray structure determined.

Introduction

The 2,2'-bipyrimidine (*bpym*) core is a versatile motif in coordination chemistry and has been used for a long time as a bridging ligand for the synthesis of homodinuclear,[1] heterodinuclear[2] or coordination networks[3,4,5] with rich spectroscopic,[6,7,8,9] electronic and magnetic properties.[10,11,12,13,14] In particular, heterodinuclear *d-f* complexes of the molecular formula $[L_2Pt(\mu\text{-}bpym)Ln(hfac)_3]$ (Ln = Yb, Nd, Er) have been designed by Ward and collaborators, showing a short intermetallic distance across the bipyrimidine bridge (6.3 Å), which leads to an efficient sensitization of the Ln NIR luminescence by the *d*-block unit, due to an energy transfer from the ^{3}MLCT state to the Lanthanide (Ln) excited state. Similarly, Seitz and coworkers used the bipyrimidine motif to construct highly stable homo- and heterodinuclear cryptate based Ln complexes.[15] Alternatively, Hemmer and co-workers synthesized bipyrimidine-based homo- and hetero-dinuclear Eu/Tb complexes and demonstrated that the *bpym* bridge was highly efficient in promoting inter-lanthanide energy transfer.[7] 2,2'-bipyrimidine is also very useful in the elaboration of lanthanide dimers with Single-Molecule Magnets (SMMs) properties, in particular with Dy(III).[11,12] In the search for new hetero-polynuclear Ln architectures to be used as photon converters for up- or down-conversion studies,[16,17,18,19] we were interested in the synthesis and

coordination study of the hexadentate analogue, 2,2'-bipyrimidine-4,4'-dicarboxylic acid (*bpd*). Since its first publication by Lehn and Regnouf De Vains,[20] the coordination chemistry of *bpd* has remained largely unexplored.

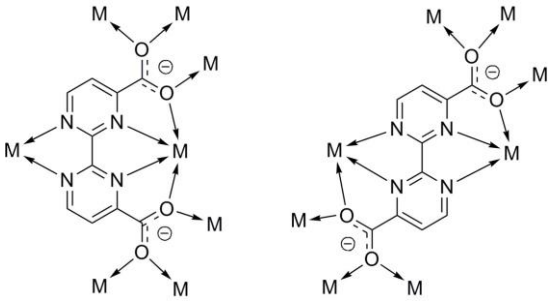

Figure 1: The possible coordination modes of 2,2'-bipyrimidine-4,4'-dicarboxylate (*bpd*).

Depending on the respective orientation of the carboxylate functions, the bpd^{2-} unit can bridge metal centers in various chelating modes: bidentate, tridentate and tetradentate (Figure 1) providing an interesting interplay between soft and hard complexing sites.[21] Within the frame of this study, we have investigated the coordination behavior of *bpd* with some Ln cations, as well as the possibility to direct the formation of polynuclear species in an attempt to control a hierarchical assembly by coordinating $[Ln(tta)_3]$ entities with the isolated Ln complexes of *bdp*.

Experimental Section

General Methods. Solvents and starting materials were purchased from Sigma-Aldrich, Acros, Carlo Erba, abcr GmbH, Fluka and Alfa Aesar and used without further purification. Flash column chromatography was performed with silica gel (10-63 μm, Macherey-Nagel). IR spectra were recorded on Agilent Technologies Cary 630 FTIR spectrometer. Elemental analyses were performed at the Plateforme Analytique des Inorganiques (REPSEM, UMR 7178 du CNRS) at ECPM, Strasbourg, France. Mass spectrometry analyses were recorded at the Service de Spectrométrie de Masse (Université de Strasbourg) on MicroTOF Bruker spectrometers equipped with an electrospray source. The spectra were recorded in negative and positive modes, depending on the nature of the samples. The ^1H NMR spectra were recorded on 300 MHz, 400 MHz or 500

MHz Bruker Avance spectrometers. The ^{13}C NMR spectra and 2D spectra, were recorded on Bruker Avance III HD - 500 MHz. Chemical shifts are reported in ppm, with residual protonated solvent as internal reference.[22] When unspecified, coupling constants refer to H-H coupling.

X-ray Crystallography. The single crystal X-ray diffraction measurements were performed on APEXII (compound (1), (2), (3) and (5)) or on D8 Venture Bruker-AXS (compound (4) and (6)) diffractometers with Mo-Kα radiation (λ = 0.71073 Å) radiation. Cell parameters refinement and data reduction were carried out with SAINT, a correction for absorption (SADABS) was applied. The structures were solved by direct methods (SIR97)[23] or by dual-space methods (SHELXT)[24] and then refined with full-matrix least-square methods based on F^2 (SHELXL-2014)[24] with the aid of the WINGX program.[25] All non-hydrogen atoms were refined with anisotropic atomic displacement parameters with exceptions for (4), (5) and (6) (see details in SI), H atoms were finally included in their calculated position. The structural Figures presented in the main part of the article were produced in Mercury.

Spectrophotometric Studies. All the stock solutions were prepared by weighing solid products on a Mettler Toledo Excellence XS series microbalance with 0.01mg readability. Distilled water (purified on a bed of ion-exchanger and activated carbon from Bioblock Scientific) or deuterated solvents (Sigma-Aldrich) were used. The lanthanide salts solutions were prepared from their chloride salts ($LnCl_3.6\ H_2O$, 99,9%, Sigma-Aldrich). The pH of the solution was determined with a Mettler Toledo pH-meter (Education line EL20) previously calibrated with buffered solution at pH 4.00 and 7.00 (Fixanal buffer, Fluka). UV-vis absorption spectra were recorded at room temperature on a Perkin-Elmer lambda 950 spectrometer and Analytic Jena Spectrometer in quartz Suprasil cuvettes with a 1 cm optical path (Helma Analytics). Steady state emission spectra were recorded on an Edinburgh Instrument FLP920 spectrometer working with a continuous 450W Xe Lamp and a red sensitive R928 photomultiplier from Hamamatsu in Pelletier housing for visible

detection (230 to 900 nm). All spectra were corrected for the instrumental functions. For emission spectra upon UV excitation, a 399 nm cutoff filter was used to eliminate second order artifacts. Phosphorescence lifetimes were measured on the same instrument working in the Multi-Channel Spectroscopy (MCS) mode, using a Xenon flash lamp as the excitation source. The errors on the lifetimes are estimated to 10%.

Synthesis

$[Lu(tta)_3(H_2O)_2]$. In a round bottom flask (150 mL) equipped with a magnetic stirring bar, 188 mg of $LuCl_3 \cdot 6H_2O$ (0.48 mmol) and 320 mg of 2-thenoyltrifluoroacetone (1.44 mmol) was dissolved in 57 mL of absolute ethanol. The pH of the solution was adjusted to 6.50 with NaOH solution in EtOH:H_2O (10:1 by volume). The reaction mixture was refluxed overnight, the precipitated solid (NaCl) was separated by filtration and the solution was evaporated to yield a yellow oil. The oil was dissolved in 7 mL of CH_2Cl_2, mixed with a portion of 57 mL of pentane and left aside for crystallization in a plugged flask. After 24 h the slightly-yellow crystalline powder was filtered-off and vacuum dried. Yield 300 mg (71%). Elemental analysis (CHN%) calculated for $[Lu(tta)_3(H_2O)_2]$, $C_{24}H_{16}F_9O_8S_3Lu$, 874.53 g/mol: C, 32.96; H, 1.84; S, 11.00; found: C, 32.80; H, 1.76; S, 10.81. ^{1}H NMR (400 MHz, Methanol-d_4) δ 7.75 (dd, J = 3.8, 1.2 Hz, 3H), 7.64 (dd, J = 4.9, 1.1 Hz, 3H), 7.09 (dd, J = 5.0, 3.8 Hz, 3H), 6.31 (s, 3H). ATR-FTIR (cm^{-1}): 684s, 751m, 771m, 789s, 860m, 933s, 1062s, 1080s, 1119vs, 1184s, 1293s, 1354s, 1408s, 1457m, 1560m, 1586s, 1653vw, 1685vw, 1696vw, 3746vw. UV-vis in MeOH: λ, nm, [$\lambda(\varepsilon)$, $M^{-1}cm^{-1}$]: 338 [11600], 269 [3670]. MS (positive ESI; MeOH) : *m/z* = 860.90 $Na^+ \cdot [Lu(tta)_3]^+$; 1698.83 $Na^+ \cdot [Lu(tta)_3]_2^+$.

H_2*bpd* $\cdot$ $3H_2O$. 120 mL of NH_3 purged and distilled *N*,*N*-dimethylformamide, 6.00 g (46.6 mmol) of 2-chloro-4-methyl pyrimidine, 12.2 g (41.8 mmol) of triphenylphosphine, 1.52 g (11.9 mmol)

of zinc powder and 1.52 g (5.94 mmol) of nickel(II) chloride were mixed in a Schlenk vessel under Ar protection at 70°C. The progress of the reaction was monitored by TLC (SiO_2 plates) in a MeOH/ethyl acetate 2:8 solvent system. After 48 h, the reaction mixture was cooled and poured into 150 mL of 2 M ammonia in water, and refrigerated (5°C) for 1h. The resulting precipitate was filtered over celite. 1.70 g of EDTA was then added to the filtrate and, after 1h, the reaction mixture was extracted with 350 mL dichloromethane. The product was purified by column chromatography on silica gel and MeOH/Ethyl Acetate 2:8 solvent system. Yield 3.0 g (70%). ^{1}H NMR ($CDCl_3$, 400 MHz): 8.82 (d, 2H), 7.24 (d, 2H), 2.69 (s, 6H). Step two. 4,4'-dimethyl-2,2'-bipyrimidine (0.97 g, 5.2 mmol) was dissolved in 220 mL of H_2O and heated at 90°C to obtain a clear orange solution. Subsequently, 20 mL of an aqueous solution of KOH (0.25 M) was added in one portion, and then a solution of $KMnO_4$ (110 mL, 0.19 M) was added in subsequent portions. The progress of oxidation was monitored by reversed phase TLC (MeCN/H_2O 80:20). After 12h, a new portion of KOH (0.2 g) and $KMnO_4$ (1.0 g) was added. After 36h, the reaction was quenched by addition of EtOH (3 mL), cooled to r.t. and filtered over celite. The filtrate was acidified with 5 M HCl to reach pH 1.6 and yielded to the precipitation of a colorless powder which was collected by vacuum filtration and dried at 90°C in vacuo. Yield 0.84 g (55%). Elemental analysis (CHN%) calculated for $H_2bpd\cdot 3H_2O$, $C_{10}H_{12}N_4O_7$, 300.66 g/mol: C, 40.01; H, 4.03; N, 18.66; found: C, 40.64; H, 3.40; N, 18.66. ^{1}H NMR (400 MHz, DMSO-d_6) δ 8.14 (d, J = 5.0 Hz, 2H), 9.28 (d, J = 5.0 Hz, 2H). ATR-FTIR (cm^{-1}): 703s, 738vs, 833w, 874m, 999m, 1044s, 1185s, 1226s, 1318s, 1357s, 1429w, 1474w, 1554s, 1700s, 3213w, 3336w. MS (negative ESI; H_2O): *m/z* = 245.03 ($Hbdp^-$); 122.01 (bdp^{2-}).

$[K_2(bpd)(H_2O)_2]$ **(1)**. 30 mg of $H_2bpd\cdot 3H_2O$ (0.10 mmol) in 10 mL of water was solubilized by addition of an aliquot of 0.8 ml of KOH in ethanol (0.3 M). The solution was then evaporated to

dryness, yielding 42 mg of white powder, which was dissolved in 1.5 mL of water and, after slow evaporation, the solid was collected by centrifugation, washed with EtOH and dried in vacuum. Yield 25 mg (68%), colorless crystalline solid insoluble in ethanol, methanol, acetonitrile and diethyl ether. Single crystals suitable for X- ray diffraction were obtained by subsequent recrystallization from water. Elemental analysis (CHN%) calculated for K_2*bpd* · $2H_2O$, $C_{10}H_8N_4O_6K_2$, 358.39 g/mol: C, 33.51; H, 2.25; N, 15.63; found: C, 33.50; H, 2.41; N, 15.53. ^{1}H NMR (400 MHz, D_2O) δ 9.14 (d, J = 5.1 Hz, 2H), 8.04 (d, J = 5.2 Hz, 2H). ATR-FTIR (cm^{-1}): 675s, 706s, 747vs, 820m, 852m, 889m, 995m, 1077m, 1187m, 1213m, 1336s, 1372s, 1426m, 1541s, 1608s, 1634s, 3094w, 3213w, 3243w, 3362w. UV-vis in H_2O: λ, nm, [$\varepsilon(\lambda)$, $M^{-1}cm^{-1}$]: 245 [17800]. MS (positive ESI; H_2O): *m/z* = 284.99 $[K(H_2bdp)_2]^+$.

$[K(H_2O)_2][Lu(bpd)_2]$ **(2)**. 14.8 mg of **(1)** (4.13×10^{-5} mol) was dissolved in 2 mL of milliQ water, then 50.0 μL of aqueous solution of $LuCl_3$·6 H_2O (0.197 M) was added (9.85×10^{-6} mol). The mixture was left for crystallization at room temperature. After two weeks, colorless rhombic crystals crystalized, which were of sufficient quality for X-ray diffraction experiment.

$[HNEt_3][Lu(bpd)_2]$ · $2H_2O$ **(3)**. 60 mg of H_2bpd·$3H_2O$ (0.20 mmol) were suspended in 10 mL of ethanol in a round bottom flask (25 mL) equipped with a magnetic stir bar and solubilized by addition of triethylamine (182 mg, 1.80 mmol). Subsequently, a solution of $LuCl_3$·$6H_2O$ (39 mg, 0.10 mmol) in 4 mL of ethanol was added in portions within 10 min under stirring. The clear solution was then evaporated to yield 132 mg of a white powder which was dissolved in methanol and precipitated from diethyl ether to yield a white precipitate, which was collected by filtration and vacuum dried. Yield 59 mg (68%). The single crystals of $[HNEt_3][Lu(bpd)_2]$·$2H_2O$, suitable for X-ray diffraction experiment, were obtained by recrystallization of the product from hot methanol. Elemental analysis (CHN%) calculated for $[HNEt_3][Lu(bpd)_2]$·$2H_2O$, $C_{26}H_{28}N_9LuO_{10}$,

801.52 g/mol: C, 38.96; H, 3.52;N, 15.73; found: C, 39.45; H, 3.29; N, 15.54. ^{1}H NMR (400 MHz, D_2O): δ 9.57 (d, J = 5.1 Hz, 4H), 8.29 (d, J = 5.1 Hz, 4H), 3.22 (q, J = 7.3 Hz, 6H), 1.33 (t, J = 7.3 Hz, 9H). ATR-FTIR (cm^{-1}): 681m, 740s, 791m, 814w, 859w, 884w, 1036w, 1073w, 1092w, 1167w, 1409m, 1459w, 1508vw, 1551s, 1636s, 1654s, 2511vw, 2693vw, 3003vw. UV-vis in MeOH: λ, nm, [ε(λ), $M^{-1}cm^{-1}$]: 255 [15000]. MS (ESI^+; H_2O): *m/z* = 665.00 $[H_2Lu(bdp)_2]^+$.

$[C_{18}H_{39}NH][Lu(bpd)_2] \cdot 0.2\ Et_3N$ **(3b)**. 12 mg (0.015 mmol) of $[HNEt_3][Lu(bpd)_2] \cdot 2H_2O$ were dissolved in 20.0 mL of trihexylamine (48.0 mg, 0.178 mmol in 100.0 mL) solution in methanol. After vacuum distillation of the amines, the residue of composition $[C_{18}H_{39}NH][Lu(bpd)_2] \cdot 0.2\ Et_3N$ was soluble in chloroform and used without further purification for spectroscopic and crystallization studies. ^{1}H NMR (400 MHz, $CDCl_3$): δ 9.39 (d, J = 4.9 Hz, 4H), 8.21 (d, J = 4.9 Hz, 4H), 2.64-2.50 (m, 6H), 1.44-1.28 (m, 6H), 1.23 (t, J = 7.1 Hz, 6H), 1.18-1.08 (m, 6H), 1.00-1.06 (m, 6H), 0.86 (t, J = 7.2 Hz, 9H). MS (negative ESI; CH_2Cl_2) m/z: 662.99 $[Lu(bdp)_2]^-$.

$[enH_2][Et_3N]_2[Lu(bpd)(tta)_2]_2 \cdot 2CHCl_3$ **(5).** 8.7 mg of $[Lu(tta)_3(H_2O)_2]$ and 13.8 mg of $[HNEt_3][Lu(bpd)_2] \cdot 2H_2O$ **(3)** were dissolved in 4 mL of methanol with 0.2 mL Et_3N and 0.2 mL ethylenediamine. A clear yellow solution was obtained after dissolution of reagents. Solvent has been evaporated at 40°C and 13 mbar to yield a yellow solid. The solid has been washed with cold chloroform and dried in vacuo. Recrystallization of the product in dry chloroform gave single crystals suitable for X-ray diffraction analysis. Yield: 15.4 mg. MS (negative ESI; CH_2Cl_2): *m/z* = 860.94 $[Lu(bpd)(tta)_2]^-$.

$[enH]_4[Lu_8(bpd)_4(tta)_{18}$ **(6)**. 8.72 mg (0.011 mmol) of $[HNEt_3][Lu(bpd)_2] \cdot 2H_2O$ and 17.47 mg (0.020 mmol) of $[Lu(tta)_3(H_2O)_2]$ were dissolved in 4.5 mL of MeOH and 0.4 mL of ethylenediamine. The solution was mixed and evaporated on the rotary evaporator to yield a yellow

glass (24.80 mg). The glass has been recrystallized in dry chloroform to yield a mixture of single-crystals. For one set of crystals, X-ray diffraction experiment was performed to give the structure of compound (6).

Results and discussion

Synthesis of the H_2*bpd* ligand and [K_2(*bpd*)(H_2O)$_2$] (1) salt

Ligand H_2*bpd* has been synthesized in two steps and 38% overall yield starting from commercially available 2-chloro-4-methylpyrimidine (Scheme 1). The bipyrimidine ring was first synthesized by Tiecco coupling in presence of triphenylphosphine, zinc powder and nickel chloride, according to the previously described procedure of Lehn and Regnouf De Vains.[20]

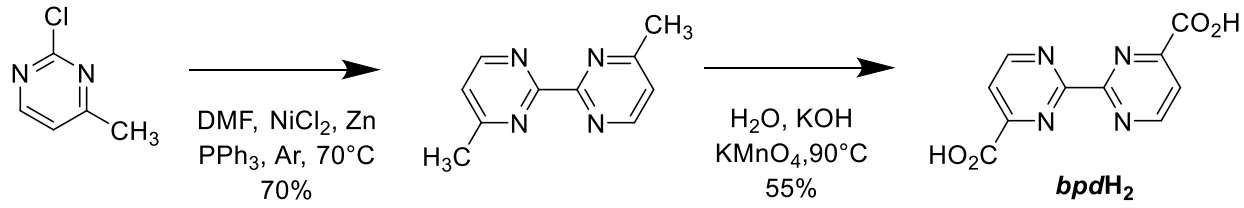

Scheme 1. Synthesis of ligand H_2*bpd*.

After oxidation of the methyl groups with $KMnO_4$ and deprotonation of the diacid by KOH, a potassium salt is obtained which is well soluble in water. Upon slow evaporation, a [K_2(*bpd*)(H_2O)$_2$] compound (1) crystallizes in a triclinic crystal system and P-1 space group. The molecular structure of (1) with the labelling of atoms is presented in Figure 2a, while crystal data and selected distances and angles are collected in Table S1-S3.

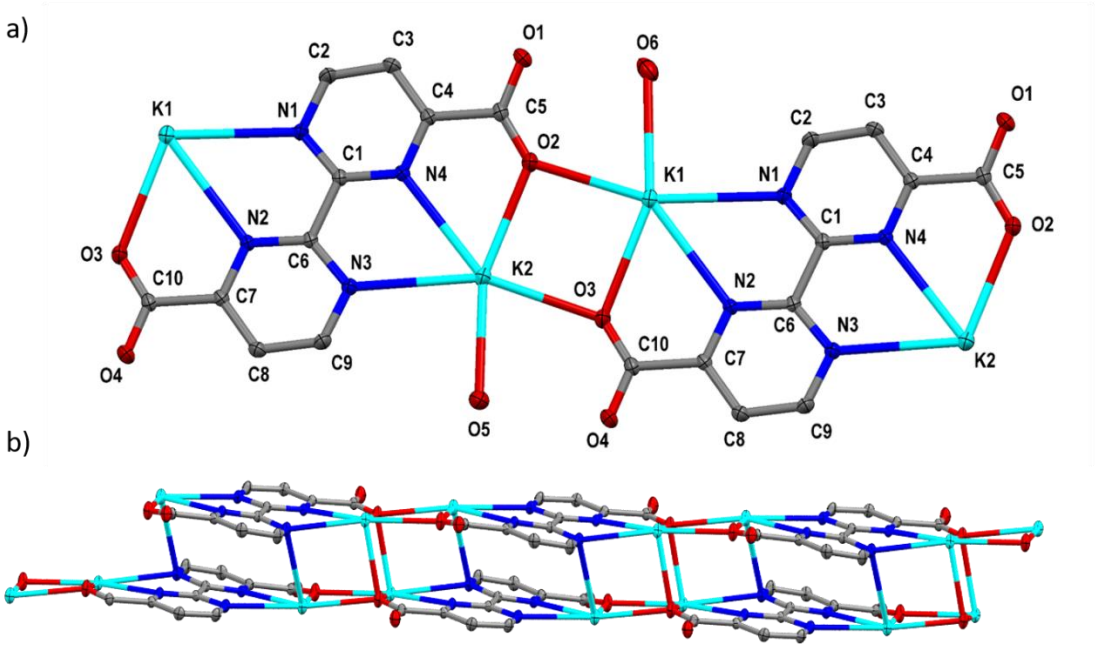

Figure 2: a) Molecular structure of $[K_2(bpd)(H_2O)_2]H_2O$ (1) at the 30% thermal ellipsoids probability. Hydrogen atoms were omitted for clarity. b) π-π stacked bilayer motif building the packing in (1).

The asymmetric unit of (1) consists of a $[K_2(bpd)(H_2O)_2]$ motif in which two potassium ions neutralise the charge of bis-tridentately coordinating bdp^{2-}. Both potassium ions K1 and K2 adopt a distorted pentagonal bipyramid geometry in which the bdp^{2-} ligand coordinates in a tridentate mode, the equatorial coordination being completed by the O atom of the water molecule and an O atom of a carboxylate function from the second ligand. The distances between the donor atoms to potassium ions span from 2.8 Å to 3.3 Å (Table S2). The bite angles of the chelating pocket κ−O, N is 1.8° larger than the κ−*N*, *N* pocket (57.2°). The distance between potassium atoms in the bridge is 7.37 Å. The $[K_2(bpd)(H_2O)_2]$ units are further joined together thanks to mono atomic bridging of the O2 and O3 atoms of the carboxylic groups as shown in Figure 2a, thereby forming a weakly undulated ribbon structure (Figure 2b). The ribbons are further assembled into supramolecular layers thanks to hydrogen bonds between the coordinated water molecule O5, and the carboxylate group at C10. The ribbons are also stabilized by the strong cation-π interaction between N1 and K2 as well as $\pi - \pi$ stacking interactions between pyrimidine carboxylate

moieties. The distance between the N3-C9-C8-C7-N2-C6 and N1-C2-C3-C4-N4- C1 planes is 3.3 Å and the angle between planes is 5.5°. The salt is highly soluble in water and thus is a convenient substrate for further coordination studies with lanthanide ions in aqueous solutions.

Study of the coordination of *bpd*$^{2-}$ and [K_2(*bpd*)(H_2O)$_2$] with lanthanide ions (Ln = Lu, Eu, Tb)

^{1}H NMR titration of [K_2(*bpd*)(H_2O)$_2$] (1) with $LuCl_3$. The coordination between the title ligand in salt (1) and lutetium chloride was monitored by a ^{1}H NMR spectroscopic titration experiment in deuterium oxide (Figure 3).

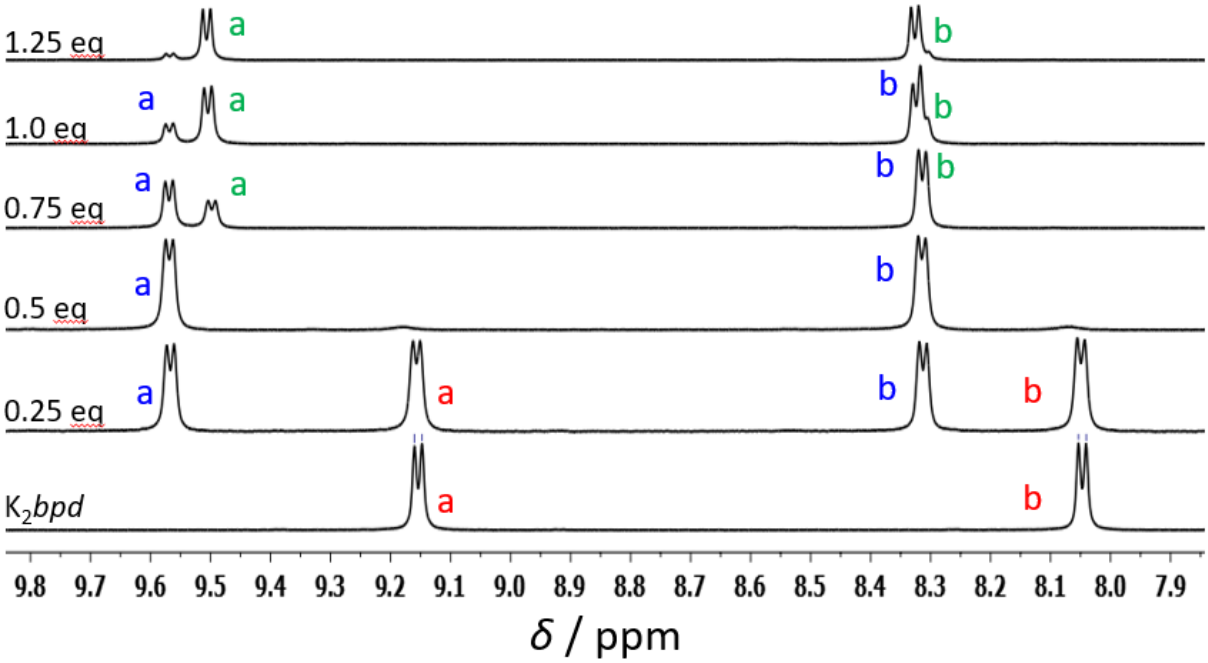

Figure 3: ^{1}H NMR spectra of the titration of [K_2(*bpd*)(H_2O)$_2$] (1) upon addition of 0 to 1.25 equiv of $LuCl_3$.6 H_2O (D_2O, [*bdp*$^{2-}$] = 0.18 mM, 400 MHz).

The solution of (1) in D_2O displays two doublets at 8.04 ppm and 9.14 ppm. These resonances can be ascribed to the proton of bipyrimidine rings, accordingly, the low field doublet was assigned to the proton adjacent to pyrimidine nitrogen (H_b, Figure 4), while the high field resonance corresponds to the proton next to the carboxylic group (H_a). Upon addition of 0.25 equivalent of $LuCl_3$, a new set of doublets appears at 8.32 ppm and 9.56 ppm, respectively. These signals can be ascribed to the resonances of bipyrimidine dicarboxylate complex [Lu(*bpd*)$_2$] (Figure 4), which is indeed the only species observed at a 1:2 Lu:*bdp* ratio. Upon further addition of $LuCl_3$, the

doublet at 9.57 ppm decreased in intensity while a new doublet appeared at 9.50 ppm. This resonance corresponds to the protons H_a and it is surmised that this new signal arises from the decoordination of one *bpd* unit, hence giving rise to the formation of a hydrated [Lu(*bpd*)] complex in a *cis*-symmetrical coordination mode similar to 6-6'-dicarboxy-2,2'-bipyridine (Figure 4).[26]

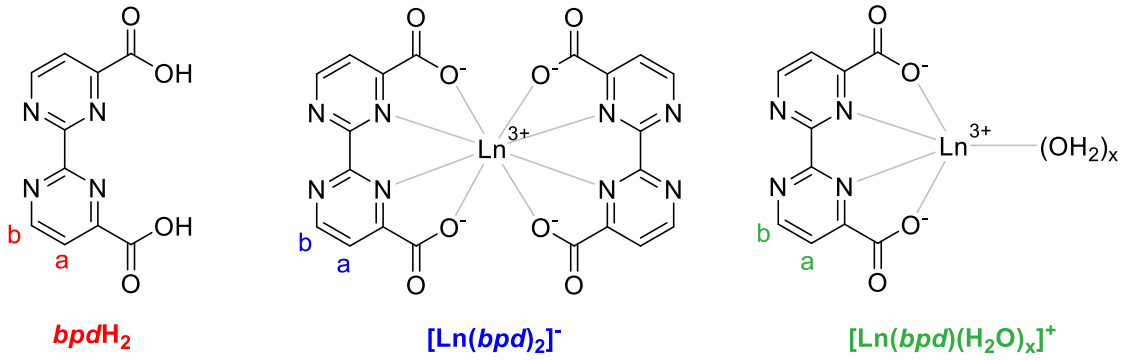

Figure 4. Schematic representation of $[Ln(bpd)_2]^-$ and $[Ln(bpd)(H_2O)_x]^+$ (Ln = Lu, Eu, Tb).

Replacing the spectroscopically silent Lu^{3+} by the visible luminescent emitters Eu^{3+} and Tb^{3+}, the coordination properties of H_2bdp could also be investigated in aqueous solution by monitoring the changes of the UV-visible absorption and steady-state emission spectra upon coordination. The complexation of $EuCl_3$ and $TbCl_3$ was studied in H_2O/DMSO mixtures (90/10) with a Tris-HCl 0.01M buffer at pH = 7.0. In these conditions, the absorption spectrum of the free ligand displayed broad bands in the 242-255 nm region characteristic of $\pi \rightarrow \pi^*$ transitions of the bipyrimidine dicarboxylate moiety. Upon Eu^{3+} addition, the absorption is slightly bathochromicaly shifted, showing the formation of an isosbestic point at 249 nm from 0.1 equiv to 0.5 equiv. of added Eu^{3+}, suggesting the formation of a binuclear $[Eu(bpd)_2]^-$ complex (Figure 5a). Then, up to 2 equiv. of metal salt added, a hypochromic shift is observed and the inflection point, observed in the absorbance monitored at 244 nm and 262 nm around one equivalent (Figure 5d), suggests the formation of a $[Eu(bpd)]^+$ species. Excitation in the *bpd* ligand at 264 nm, led to the typical $^5D_0 \rightarrow {}^7F_J$ (J = 0 – 4) transitions of Eu^{3+} (Figure 5b)[27] with a maximum intensity recorded in presence of

0.5 equiv of Eu^{3+}, hence confirming the formation of the $[Eu(bpd)_2]^-$ species and its optimal sensitization. Assuming a bis-tetradentate coordination mode of the *bpd* ligands afforded an octacoordination of the Eu atom and a strong shielding towards water molecules and their luminescence quenching effects.[28] Further addition of Eu^{3+} led to the formation of the $[Eu(bpd)]^+$ species with a strong decrease of the emission intensity (Figure 5d) up to *ca* one equivalent, followed by a plateau region for further additions. This behavior strongly supports the formation of a hydrated species, as the presence of water molecules in the first coordination sphere of Eu is expected to quench a part of the luminescence.[29] Analysis of the time decay profiles recorded at 616 nm also indicated the formation of two species: a $[Eu(bpd)_2]^-$ species with $\tau_{Eu(bpd)_2}$ = 534 μs and a hydrated $[Eu(bpd)]^+$ species, which luminescent is partially quenched by O-H vibrations of the solvent ($\tau_{Eu(bpd)}$ = 216 μs). Such speciation is also confirmed with Tb^{3+} ion, showing typical $^5D_4 \rightarrow {}^7F_J$ (J = 6 – 3) transitions[30] (Figure 5c), an inflexion point in the emission intensity at 0.5 equivalent and a maximum sensitization in presence of one equivalent of added Tb^{3+} (Figure 5d). In the case of Tb^{3+}, sensitization is most efficient for [Tb(*bpd*)] than $[Tb(bpd)_2]$, which most probably arises from the presence of a $Tb^{3+} \rightarrow {}^3T^*$(*bdp)* back energy transfer, as confirmed by the time-decay measurements of the two species ($\tau_{Tb(bpd)_2}$ = 170 μs and $\tau_{Tb(bpd)}$ = 581 μs).

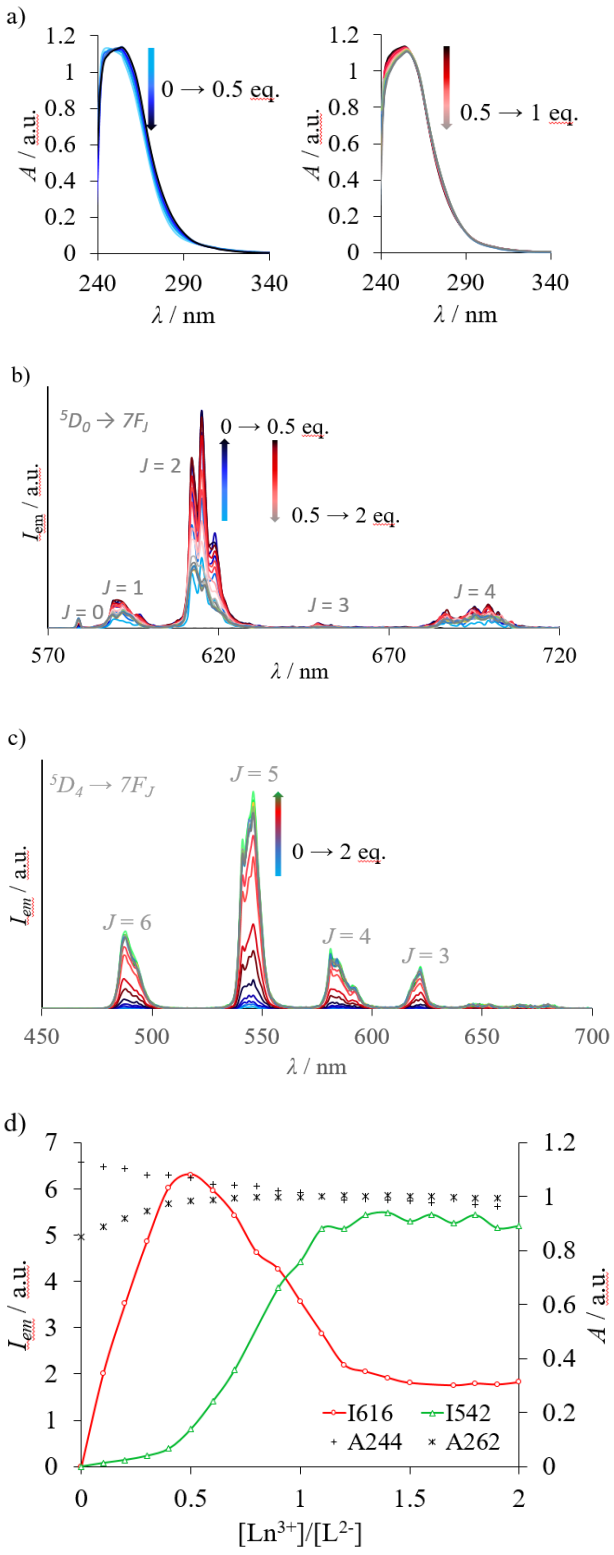

Figure 5: Evolution of the absorption (a, Ln = Eu) and emission (b, Ln = Eu; c, Ln = Tb) spectra of a solution of H_2*bpd* in 0.01M Tris-HCl (7×10^{-5} M, pH = 7.0, λ_{exc}= 264 nm) upon addition of aliquots of $LnCl_3.6H_2O$. (d) Evolution of the luminescence intensity at 616 nm and 545 nm and of

the absorbances at 244 and 262 nm as a function of the [Ln]/[bpd^{2-}] ratio.

Considering the results obtained from ^{1}H NMR, spectrophotometric and spectrofluorimetric titrations, it was attempted to isolate the [Lu(*bpd*)$_2$]$^-$ complex from an aqueous solution containing $LuCl_3$ and K_2*bpd* in a 1:2 molar ratio. Colorless prism crystals of suitable size and quality for single-crystal X-ray diffraction experiment, were grown, corresponding to the potassium salt [K(H_2O)$_2$][Lu(bpd)$_2$] (2) (Figure 6). The crystal data and selected experimental details for compound (2) are given in Table S1 while selected bond distances and angles are given in Table S4 and Table S5.

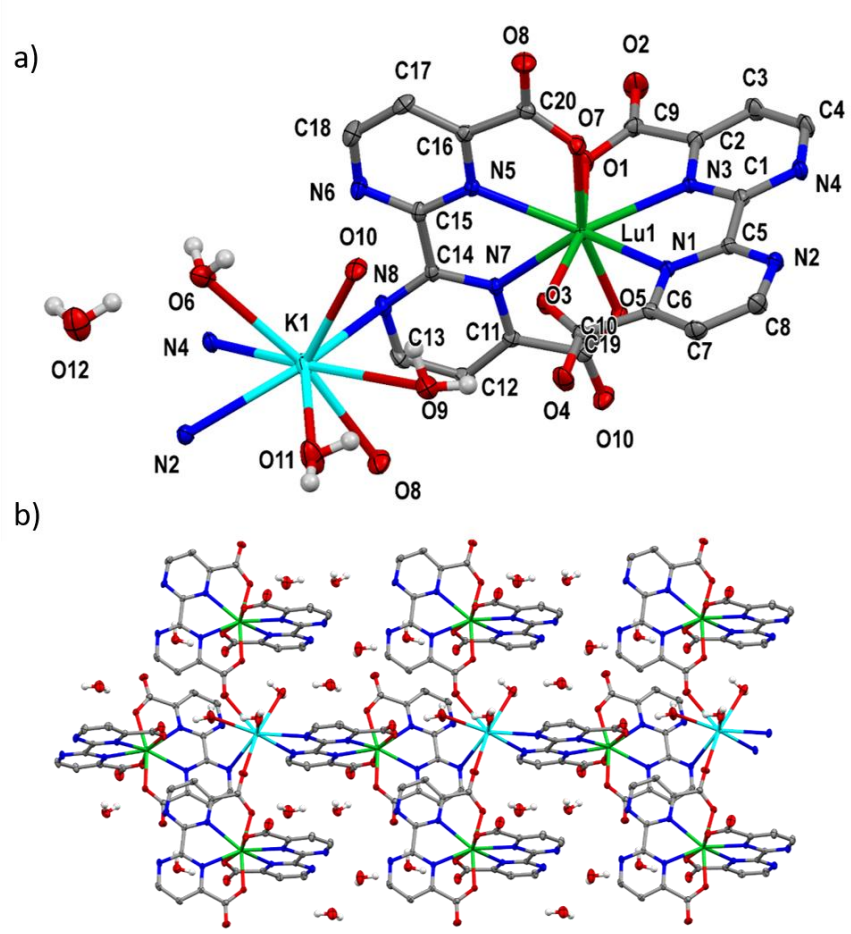

Figure 6: a) Molecular structure of [K(H_2O)$_2$][Lu(*bpd*)$_2$] (2) at the 30% thermal ellipsoids probability. Hydrogen atoms were omitted for clarity except for H_2O molecules. b) View of the extended layer structure.

In compound (2), the lutetium(III) ion is coordinated by two tetradentate bpd^{2-} ligands, to form an

anionic $[Lu(bpd)_2]^-$ complex with two *κ-N,N* bidentate sites. The first bidentate site is occupied by the Lu(III) atom, which is also coordinated by the two carboxylate functions, and the second site is occupied by the potassium cation K1 to compensate the charge. The geometry of the octacoordinated lutenium was analyzed with the Shape program,[31] giving the smallest shape deviations for the triangular dodecahedron (TDD) and the Johnson snub diphenoid (J-SD)[32] polygons (shape deviation of 2.579 and 2.498 for TDD and J-SD respectively). The average Lu-N and Lu-O bonds (respectively 2.43(1) and 2.27(1) Å) are in line with those observed for the analogous Tb complex composed of two tetradentate 6,6'-carboxy-2,2'-bipyridine,[26] taking into account the ionic contraction from Lu to Tb.[33] The rest of the first coordination sphere of K1 is filled with three coordinated water molecules (O6, O9 and O11), two oxygen atoms from the carboxylate groups at C19 and C20. The dihedral angle between the mean planes of the tetradentate ligands is 83.3 Å. The crystal packing of salt (2) results in the formation of layers which are joined by weak to medium hydrogen bonds with water molecules. In particular, the carboxylate groups at C19 and C20 act as a bridge through hydrogen bonding interactions with water molecules H_2O6 and H_2O9. Donor-acceptor distances amount to $d_{D\text{-}A}$ = 2.813 Å, D-Ĥ-A = 171.5° for H_2O6 and O5, $d_{D\text{-}A}$ = 2.838 Å, D-Ĥ-A = 152.4° for H_2O9 and O10 and $d_{D\text{-}A}$ = 2.801 Å, D-Ĥ-A = 176.5° for H_2O9 and O4. In addition, a cation-π interaction is observed between K1 and N8 from the pyrimidine ring.

Interactions between $[Lu(bpd)_2]^-$ and $[Lu(tta)_3(H_2O)_2]$.

Considering that the $[Lu(bpd)_2]^-$ complex possesses two *exo* N-N bidentate chelating units, we hypothesized that these chelating site should be of potential interest for the coordination of further Ln^{3+} cations. In addition, $[Ln(tta)_3(H_2O)_2]$ salts are known to form a large range of ternary complexes in the presence of *N,N*-bidentate ligands.[34] The interaction of $[Lu(bpd)_2]^-$ with $[Lu(tta)_3(H_2O)_2]$ was thus investigated. However, the interaction between $[Lu(bpd)_2]^-$ and

$[Lu(tta)_3(H_2O)_2]$ building blocks require aprotic organic solvents in order to minimize O-H competitors and dissociation.[2] As the potassium salt of $[Lu(bpd)_2]^-$ is poorly soluble in non-aqueous solvents, we turned to the use of $[Lu(bpd)_2]^-$ salts with triethylammonium, trihexylammonium or ethylenediamonium counter ions, which were obtained by metathesis of the potassium salt (1). The triethylammonium salt with the formula $[Et_3NH][Lu(bpd)_2]\cdot 2H_2O$ (3) crystallizes as colorless prism crystals from water-methanol solution (1:99, V:V). The crystals possess a monoclinic unit cell with *C2/c* space group. The Lu1 center has similar coordination geometry as in the structure of (2). Bond distances and angles are presented in Table S6 and Table S7, respectively. The molecular structure of the crystal with the labelling of the atoms is shown in Figure 7.

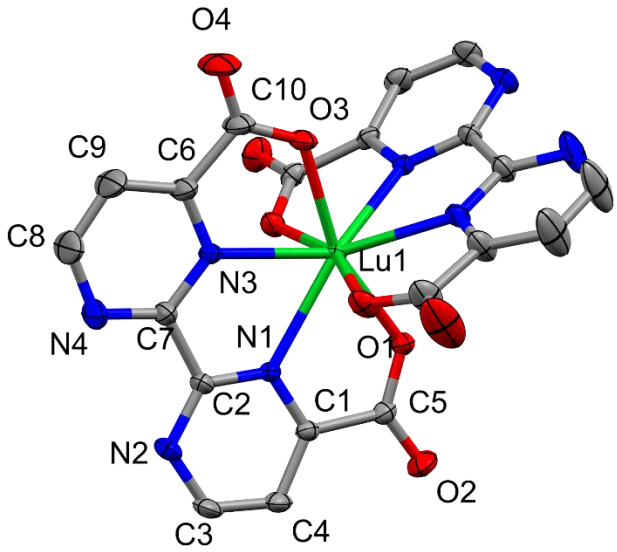

Figure 7: Molecular structure of compound (3) at the 30% thermal ellipsoids probability.

The lutetium atom is coordinated by two tetradentate ligands through N and O donors. The Shape analysis of the coordination sphere of the lutetium gives the smallest shape deviations for the triangular dodecahedron (TDD) and the Johnson snub diphenoid (J-SD)[32] polygons (shape deviation of 2.423 and 2.478 for TDD and J-SD respectively). Surprisingly, the angle between the

planes of the *bpd* pyrimidine rings of the two ligands is far from the normal angle with a value of 75°. This is in marked contrast with the angle observed for the potassium salt (2) (82.7°) or even with the Tb analogue with 6,6'-dicarboxy-2,2'-bipyridine ligands (angle of 88.5°). Here again, both medium and weak hydrogen bonds as well as $\pi - \pi$ stacking interactions between pyrimidine rings are responsible for the assembly in the lattice.

In order to study the coordination behavior of the *exo-N,N* bidentate site of compound (3), the addition of aliquots of $[Lu(tta)_3(H_2O)_2]$ into a $[(Et_3NH)Lu(bdp)_2]$ solution was monitored by ^1H NMR (Figure 8). For solubility reasons, deuterated methanol was used and the additions were limited to 1.0 equivalent.

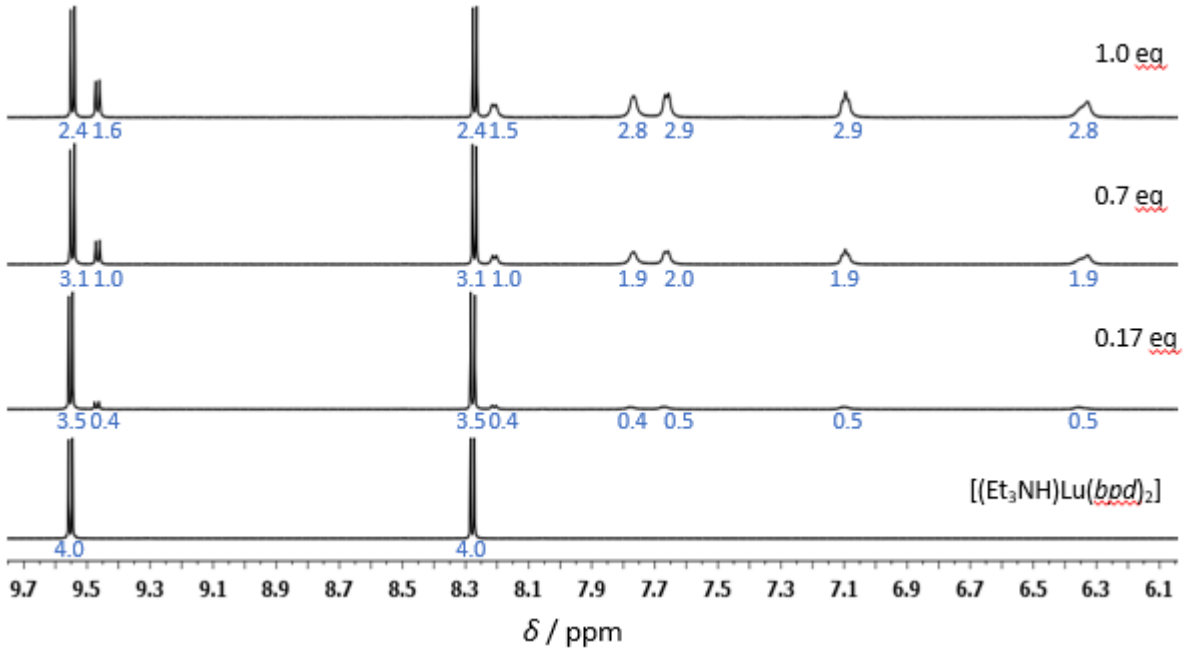

Figure 8: Aromatic region of the ^1H NMR spectra of $[(Et_3NH)Lu(bpd)_2]$ (3) upon addition of 0 to 3 equiv of $[Lu(tta)_3(H_2O)_2]$ (CD_3OD, 400 MHz, r.t.). Integral values are displayed in blue.

In solution, the displacement of the two water molecules of $[Lu(tta)_3(H_2O)_2]$ by $[Lu(bpd)_2]^-$ is not as easy as when using 2,2'-bipyridine or 1,10-phenanthroline ligands.[35] Indeed, the thermodynamic stability constant is expected to be significantly lower with less basic *bpym* and *bpd* ligands.[2] Nevertheless, a new set of signals at 8.20 and 9.46 ppm confirms the formation of a

new *bpd* species in solution. In parallel, the signals of the [Lu(tta)$_3$] complex remain also almost unaffected, except for signal broadening and the presence of a shoulder on the peak observed at 6.31 ppm. Considering the observation of only a pair of new doublets in the NMR titration, the formation of a [Lu(*bpd*)$_2$Lu(tta)$_3$] complex can be discarded in such conditions. In contrast, symmetrical species such as [Lu(tta)$_3$Lu(*bpd*)$_2$Lu(tta)$_3$] (in which two [Lu(tta)$_3$] units are coordinated to the *exo-N,N* bidentate sites) or [Lu(*bpd*)(tta)$_3$] can be envisaged, as well as other species in which the *bpd* units are related by an element of symmetry in the complex. The answer was obtained by slow evaporation of an ethanolic solution, affording single crystals suitable for X-ray diffraction analyses. The structure of a dimeric neutral compound [Lu$_2$(*bpd*)(tta)$_4$] could be refined from a set of twin crystals. The tta to *bdp* ratio in this structure (4:2) is in perfect agreement with the ^{1}H NMR integrals measured in presence of 0.7 and 1.0 equiv of [Lu(tta)$_3$(H$_2$O)$_2$]. The ethanol-aqua solvate of the formula [Lu$_2$(*bpd*)(tta)$_4$(EtOH)$_2$]·EtOH·H$_2$O (4) crystallizes in the monoclinic crystal system and *P* 2$_1$ space group (Figure 9). The crystal data and experimental details are presented in Table S12. Corresponding distances and angles are given in Table S8 and S9.

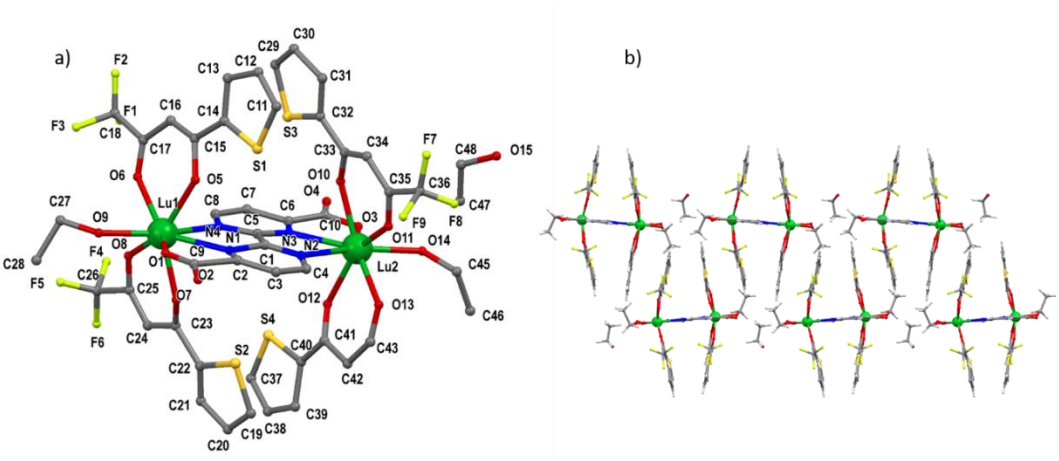

Figure 9: a) Ball and stick representation of the crystal structure of the complex (4). b) representation of crystal packing along b axis.

The Shape analysis of the two octacoordinated lutetium center show geometries close to the idealized

triangular dodecahedron31, 32 geometry with shape deviation of 1.247 and 0.810 for Lu1 and Lu2 respectively. The *bpd* ligand adopts a *trans* conformation while chelating in a bis-tridentate manner to the Lu^{3+}. Two *tta* and one ethanol molecule complete the coordination sphere of each of the metal centers. The *tta* ligands are almost perpendicular to the bipyrimidine ring. The ethanol molecule acts as bridging entity to the carboxylate function of another symmetrically equivalent diad molecule, thus forming supramolecular chains. These chains are then arranged thanks to $\pi - \pi$ stacking interactions between aromatic planes of *tta* ligands in a manner resembling a zip in the up and down directions with respect to the *bpd* plane (Figure 9b). These supramolecular layers are then arranged in space based only on weak interactions, between trifluoromethyl groups and bipirimidine rings. Noteworthy, the solubility of the diad is poor in most of organic solvents except dimethyl sulfoxide.

Upon forcing the basic conditions by addition of ethylenediamine, a mononuclear heteroleptic complex could be crystallised as an ethylenediammonium salt of formula $[enH][Lu(bpd)(tta)_2]\cdot 2CHCl_3$ (5) (Figure 10). The molecular structure of (5) is presented in Figure 10, while the selected bond distances and angles are given in Table S10 and Table S11.

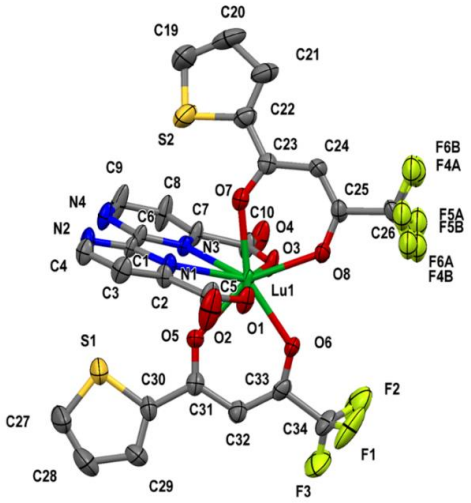

Figure 10: Molecular structure of compound (5) at the 30% thermal ellipsoids probability.

Compound (5) crystallizes in a monoclinic crystal system and $P\,2_1/c$ space group. The *bpd* ligand coordinates to lutetium in a tetradentate mode and *cis* conformation. Considering the *bpd* plane as the horizontal plane, two *tta* units are coordinated vertically in a bidentate mode, hence forming aromatic six-membered chelate rings. Interestingly, the thienyl rings are oriented in a *cis* fashion to each other, with sulfur atoms pointing towards the bipyrimidine ring. The *exo* N-N bidentate chelating sites of the *bpd* rings are involved in hydrogen bonding interactions with the ethylenediammonium cation, disordered over two sites. The carboxylate groups are surrounded by two chloroform molecules in a weak hydrogen bonding interaction, both above and below the horizontal plane of the molecule.

The final step of this study was directed towards the use of non-coordinating solvents such as chloroform with the aim to further enforce the interaction between $[Lu(tta)_3(H_2O)_2]$ and the *exo* diimine of *bpd* and to prevent the partial decoordination of $[Lu(bpd)_2]$. Since the poor solubility of the salt (3) prevented this experiment, the triethylammonium cation was exchanged into a trihexylammonium one. In a similar manner as when ethylenediamine is used, very good solubility was achieved, affording the possibility to register the ^{1}H NMR spectra and to follow the titration with $[Lu(tta)_3(H_2O)_2]$ such as presented in Figure 11.

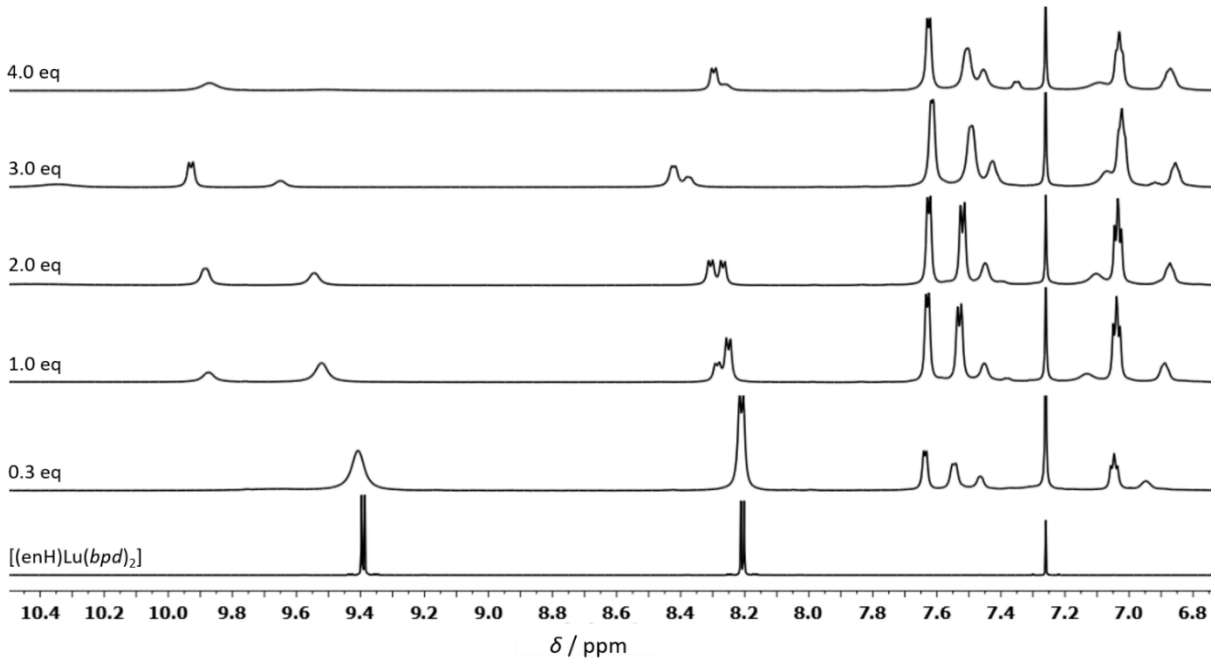

Figure 11: ^{1}H NMR titration of [(Hex$_3$NH)Lu(*bpd*)$_2$] salt (3b) by [Lu(tta)$_3$(H$_2$O)$_2$] (CDCl$_3$, 400 MHz, r.t.).

The hexylammonium salt (3b) is well soluble in CDCl$_3$ and gives two doublets at 9.39 and 8.21 ppm, respectively. Upon incremental addition of [Lu(tta)$_3$(H$_2$O)$_2$], the sharp structures of the doublets are broadened, and from 1 equivalent of [Lu(tta)$_3$(H$_2$O)$_2$] added and above, a new set of signals is observed. In particular, the doublet at 9.39 ppm is strongly downfield shifted, which is ascribed to the coordination of the other face of the bipyridine to form supramolecular structures of larger sizes. Unfortunately, the broadening of the signals prevented an accurate determination of the stoichiometry of these adducts. In addition, electrospray mass spectrometry analysis of the assemblies was inconclusive. However, in one of such experiments, when these compounds were dissolved in chloroform in a stoichiometric ratio of 1:2, a mixture of crystals crystallized. One phase has not been identified since the crystals quickly loses solvent, but from the other phase, compound (6) could be analyzed by single crystal X-ray diffraction. Crystals of compound (6) are weakly and low angle diffracting crystals, synchrotron measurement would be more appropriate

for such sample. Nevertheless, this data collection performed on a laboratory diffractometer gave a first insight into the cluster's structure shown in Figure 12. The position of the Lu atoms and the bridging ligands were unambiguously found, the refinement of the position and thermal parameters of the chelating *β*-diketonate *tta* ligands requires the use of a lot of constraints/restraints (see cif file for the full list). This unusual number of constraint and restraint could be explained by a combination of unsolved rotational disorder of the CF_3 groups together with positional disorder of the full β-diketonate *tta* ligands. Attempts to apply such model in refinements were unsuccessful. Unidentified solvent present in the voids (36-40% of the unit cell volume) has been squeezed. The prism crystals of (6) possess a large monoclinic unit cell and the lattice belong to $P2_1/c$ space group. The crystal data and selected experimental details are presented in Table S12. Atom numbering with ellipsoid representation at 30% probability level and selected bond distances are given in the SI.

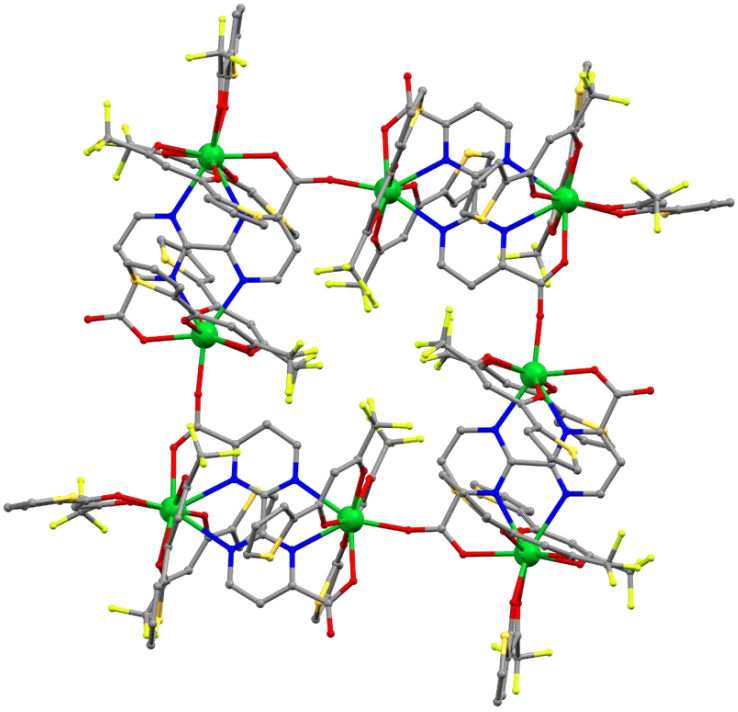

Figure 12: Ball and stick representation of the crystal structure of compound (6).

The eight lutetium atoms are linked together by four *bpd* ligands in *bis*-tridentate conformation as well as *anti-anti* bridging mode by carboxylate groups. The Lu^{3+} centers positioned in the corners of the square are nonacoordinated while the ones in the sides of the square are octacoordinated. The coordination spheres of both coordination centers are saturated with the chelating *β*-diketonate ligands. Typically, Lu-Lu distances in this structure are in the order of 6.7 Å to 6.9 Å. Although rare,[36,37] such arrangement of molecule brings eight lanthanide (here Lu) centers in close proximity and is of significant interest in a wide range of applications such as luminescence,[38,39,40,41,42], magnetism.[43,44] or quantum information processing. [45]

Conclusion

For the first time, the potential of 2,2'-bipyrimidine-4,4'-dicarboxylic acid (bpd^{2-}) ligand as building block for lanthanide coordination (Ln = Lu, Eu, Tb) has been explored. bdp^{2-} is a versatile unit, acting both as bridging and chelating ligand and a large variety of homoleptic mononuclear and heteroleptic complexes has been identified. In aqueous solutions, luminescent $[Ln(bdp)_2]^-$ have been obtained with Ln = Eu, Tb and the corresponding solid state structure of $[K(H_2O)_2][Lu(bpd)_2]$ (2) has been determined by X-ray diffraction studies on single crystals. In these complexes, the Ln(III) is octacoordinated by two tetradentate bdp^{2-} units in the *cis* conformation. Further coordination of the *exo* α-diimine to $[Lu(tta)_3(H_2O)_2]$ could be investigated in protic but also in aprotic solvents, by using the corresponding alkylamonnium salts $[(Alk\text{NH})Lu(bpd)_2]$ (*Alk* = Et, Hex, en) obtained by methathesis. Three new species have been identified: the monometallic complex $H[Lu(bpd)(tta)_2]$ (5), the dimer $[Lu_2(bpd)(tta)_4]$ (4) and the octametallic complex $[enH]_4[Lu_8(bpd)_4(tta)_{18}]$ (6), as confirmed by their solid state structure. The polynuclear assemblies are characterized by short intermetallic distances in the order of 6.5Å to

6.9Å of potential interest for Ln to Ln energy transfer processes.

Acknowledgement

This work was carried out within the framework of a project of the IPVF (Institut Photovoltaïque d'Ile-de-France). This project has been supported by the French Government within the framework of the program of investment for the future (Programme d'Investissement d'Avenir, ANR-IEED-002-01), the French Centre National de la Recherche Scientifique (CNRS), and the University of Strasbourg.

Supporting Information Available

The Supporting Information is available free of charge on the ACS Publication website at DOI: xxxx.

^{1}H NMR and ESI spectra of $H_2bpd\cdot 3\ H_2O$, of $[K_2(H_2O)(bpd)]\cdot H_2O$, $[HNEt_3][Lu(bpd)_2]\cdot 2\ H_2O$, $[C_{18}H_{39}NH][Lu(bpd)_2]\cdot 0.2\ Et_3N$, $[enH_2][Et_3N]_2[Lu(bpd)(tta)_2]_2$ (figure S1-S9); Crystal data and selected distances and angles for compound (1) – (6), Shape analysis of Lu complexes using SHAPE 2.1 software (Table S1-S14).

Accession Codes

CCDC 2072522-2072527 contain the supplementary crystallographic data for this paper. These data can be obtained free of charge via www.ccdc.cam.ac.uk/data_request/cif, or by emailing data_request@ccdc.cam.ac.uk, or by contacting The Cambridge Crystallographic Data Centre, 12 union Road, Cambridge CB2 1EZ, UK, fax: +44 1223 336033.

References

[1] Brewer, G.; Sinn, E. 2,2'-Bipyrimidine-bridged homobinuclear complexes. *Inorg. Chem.* **1985**, *24*, 4580-4584.

[2] Shavaleev, N.M.; Accorsi, G.; Virgili, D.; Bell, Z.R.; Lazarides, T.; Calogero, G.; Armaroli, N.; Ward, M.D. Syntheses and crystal structures of dinuclear complexes containing *d*-block and *f*-block luminophors. Sensitization of NIR luminescence from Yb(III), Nd(III), and Er(III) centers by energy transfer from Re(I)- and Pt(II)-bipyrimidine metal centers. *Inorg. Chem.* **2005**, *44*, 61-72.

[3] Hunziker, M.; Ludi, A. Ruthenium(II)-bipyrimidine complexes. Spectroscopic and

electrochemical properties of a novel series of compounds. *J. Am. Chem. Soc.* **1977**, *99*, 7370-7371.
[4] Castro, I.; Sletten, J.; Glaerum, L.K.; Cano, J.; Lloret, F.; Faus, J.; Julve, M. Syntheses, crystal structures and electronic properties of [Cu(bipym)(C_4O_4)(H_2O)$_3$].2H_2O and [Cu_2(*bipym*)(C_4O_4)2(H_2O)$_6$] (*bipym* = 2,2'-bipyrimidine). *J. Chem. Soc., Dalton Trans.* **1995**, *19*, 3207-13.
[5] De Munno, G.; Julve, M.; Lloret, F.; Cano, J.; Caneschi, A. Magneto-structural effects of the Jahn-Teller distortions on 2,2'-Bipyrimidine-, (*bpm*-) bridged dinuclear copper(II) complexes: Crystal structures and magnetic properties of [Cu_2(*bpm*)(H_2O)$_4$(SO_4)$_2$]·3H_2O and [Cu_2(*bpm*)(H_2O)$_8$](SO_4)2·2H_2O. *Inorg. Chem.* **1995**, *34*, 2048-2053.
[6] Zucchi, G.; Maury, O.; Thuery, P.; Gumy, F.; Bünzli, J.-C. G.; Ephritikhine, M. 2,2'-Bipyrimidine as efficient sensitizer of the solid-state luminescence of lanthanide and uranyl ions from visible to near-infrared. *Chem. Eur. J.* **2009**, *15*, 9686-9696.
[7] Errulat, D. Gabidullin,B.; Murugesu, M.; Hemmer, E. Probing optical anisotropy and polymorph-dependent photoluminescence in [Ln_2] complexes by hyperspectral imaging on single crystals. *Chem. Eur. J.* **2018**, *24*, 10146 – 10155.
[8] Richards, G.; Osterwyk, J.; Flikkema, J.; Cobb, K.; Sullivan, M.; Swavey, S. Monometallic and bimetallic europium(III) and terbium(III) complexes: Synthesis and luminescent properties. *Inorg. Chem. Commun.* **2008**, *11*, 1385-1387.
[9] Fratini, A.; Richards, G.; Larder, E.; Swavey, S. Neodymium, gadolinium, and terbium complexes containing hexafluoroacetylacetonate and 2,2'-bipyrimidine: structural and spectroscopic characterization. *Inorg. Chem.* **2008**, *47*, 1030-1036.
[10] Gould, C.A.; Mu, E.; Vieru, V.; Darago, L.E.; Chakarawet, K.; Gonzalez, M.I.; Demir, S.; Long, J.R. Substituent effects on exchange coupling and magnetic relaxation in 2,2'-bipyrimidine radical-bridged dilanthanide complexes. *J. Am. Chem. Soc.* **2020**, *142*, 21197-21209.
[11] Moreno-Pineda, E.; Taran, G.; Wernsdorfer, W.; Ruben, M. Quantum tunnelling of the magnetisation in single-molecule magnet isotopologue dimers. *Chem. Sci.* **2019**, *10*, 5138-5145.
[12] Perfetti, M.; Gysler, M.; Rechkemmer-Patalen, Y.; Zhang, P.; Tastan, H.; Fischer, F.; Netz, J.; Frey, W.; Zimmermann, L.W.; Schleid, T.; Hakl, M.; Orlita, M.; Ungur, L.; Chibotaru, L.; Brock-Nannestad, T.; Piligkos, S.; van Slageren, J. Determination of the electronic structure of a dinuclear dysprosium single molecule magnet without symmetry idealization. *Chem. Sci.* **2019**, *10*, 2101-2110.
[13] Real, J.A.; Gaspar, A.B.; Niel, V.; Munoz, M.C. Communication between iron(II) building blocks in cooperative spin transition phenomena. *Coord. Chem. Rev.* **2003**, *236*, 121-141.
[14] Real, J.A.; Bolvin, H.; Bousseksou, A.; Dworkin, A.; Kahn, O.; Varret, F.; Zarembowitch, J. Two-step spin crossover in the new dinuclear compound [Fe(*bt*)(NCS)$_2$]$_2$*bpym*, with *bt* = 2,2'-bi-2-thiazoline and *bpym* = 2,2'-bipyrimidine: experimental investigation and theoretical approach. *J. Am. Chem. Soc.* **1992**, *114*, 4650-4658.
[15] Wahsner, J.; Seitz, M. Synthesis of inert homo- and heterodinuclear rare-earth cryptates. *Inorg. Chem.* **2015**, *54*, 9681−9683.
[16] Nonat, A. M.; Charbonnière, L. J. Upconversion of Light with Molecular and Supramolecular Lanthanide Complexes. *Coord. Chem. Rev.* **2020**, *409*, 213192.
[17] Nonat, A.; Liu, T.; Elhabiri, M.; Jeannin, O.; Camerel, F.; Charbonnière, L.J. Energy transfer in supramolecular heteronuclear lanthanide dimers and application to fluoride sensing in water. *Chem. Eur. J.* **2018**, *24*, 3784-3792.
[18] Nonat, A.; Bahamyrou, S.; Lecointre, A.; Przybilla, F.; Mély, Y.; Platas-Iglesias, C.; Camerel, F.; Jeannin, O.; Charbonnière, L.J. Molecular upconversion in water in heteropolynuclear

supramolecular Tb/Yb assemblies *J. Am. Chem. Soc*. **2019,** *141*, 1568-1576.
[19]Löning, M.; Lombez, L.; Guillemoles, J.-F.; Suchet, D. A Bayesian Approach to Luminescent Down-Conversion. *J. Chem. Phys.* **2021**, *154* (1), 014201.
[20] Lehn, J.-M.; De Vains, J.-B. R. Synthesis and properties of macrobicyclic cryptates incorporating five-and six-membered biheteroaryl units. *Helv. Chim. Acta* **1992**, *75*, 1221–1236.
[21]Prodi, L.; Montalti, M.; Zaccheroni, N.; Pickaert, G.; Charbonnière, L.; Ziessel, R. New europium(III) complexes containing hybrid ligands with hard and soft complexation centres. *New J. Chem* **2003**, *27*, 134-139.
[22] Gottlieb, H.E.; Kotlyar, V.; Nudelman, A. NMR chemical shifts of common laboratory solvents as trace impurities. *J. Org. Chem.* **1997**, *62*, 7512-7515.
[23] Altomare, A.; Burla, M. C.; Camalli, M.; Cascarano, G. L.; Giacovazzo, C.; Guagliardi, A.; Moliterni, A. G.; Polidori, G.; Spagna, R., *J. Appl. Crystallogr*., **1999**, *32*, 115–119.
[24] Sheldrick G. M. *Acta Cryst*., **2015**, *A71*, 3-8.
[25] Farrugia, L. J., *J. Appl. Cryst*., **1999**, *32*, 837–838.
[26] Bünzli, J.-C. G.; Charbonnière, L.J.; Ziessel, R.F. Structural and photophysical properties of LnIII complexes with 2,2'-bipyridine-6,6'-dicarboxylic acid: surprising formation of a H-bonded network of bimetallic entities. *J. Chem. Soc. Dalton Trans.* **2000**, 1917-1923.
[27] Eliseeva, S.V.; Bünzli, J.-C. G. Lanthanide luminescence for functional materials and bio-sciences. *Chem. Soc. Rev.*, **2010**, *39*, 189–227.
[28] Beeby, A.; Clarkson, I.M.; Dickins, R.S.; Faulkner, S.; Parker, D.; Royle, L.; de Sousa, A.S.; Williams, J.A.G.; Woods, M. Non-radiative deactivation of the excited states of europium, terbium and ytterbium complexes by proximate energy-matched OH, NH and CH oscillators: an improved luminescence method for establishing solution hydration states. *J. Chem. Soc., Perkin Trans. 2*, **1999**, 493–503.
[29] Charbonnière, L.; Mameri, S.; Kadjane, P.; Platas-Iglesias, C.; Ziessel, R. Tuning the coordination sphere around highly luminescent lanthanide complexes. *Inorg. Chem.* **2008**, *47*, 3748-3762.
[30] Eliseeva, S. V.; Bünzli, J.-C. G. Lanthanide Luminescence for Functional Materials and Bio-Sciences. *Chem. Soc. Rev.* **2009**, *39* (1), 189–227.
[31] Llunell, M.; Casanova, D.; Cirera, J.; Alemany, P.; Alvarez, S. SHAPE : Program for the Stereochemical Analysis of Molecular Fragments by Means of Continuous Shape Measures and Associated Tools, Eletronic Strucutre Group, University of Barcelona.
[32] Casanova, D.; Llunell, M.; Alemany, P.; Alvarez, S. The rich stereochemistry of eight-vertex polyhedra: a continuous shape measures study. *Chem. Eur. J.* **2005**, *11*, 1479-1494.
[33] Shannon, R.D. Revised effective ionic radii and systematic studies of interatomic distances in halides and chalcogenides. *Acta Cryst.* **1976**, *A32*, 751-767.
[34] Gavriluta, A.; Fix, T.; Nonat, A.; Slaoui, A.; Guillemoles, J.-F.; Charbonnière, L. J. Tuning the Chemical Properties of Europium Complexes as Downshifting Agents for Copper Indium Gallium Selenide Solar Cells. *J. Mater. Chem. A* **2017**, *5* (27), 14031–14040.
[35] Yajima, S.; Hasegawa, Y. Variation of thermodynamic parameters in the adduct formation of *β*-diketonato chelates with 1,10-phenanthroline across the lanthanoid series. *Bull. Chem. Soc. Jpn* **1998**, *71*, 2825-2829.
[36] Kobylarczyk, J.; Kuzniak, E.; Liberka, M.; Chorazy, S.; Sieklucka, B.; Podgajny, R. Modular Approach towards Functional Multimetallic Coordination Clusters. *Coord. Chem. Rev.* **2020**, *419*, 213394.
[37] Zheng, X.-Y.; Xie, J.; Kong, X.-J.; Long, L.-S.; Zheng, L.-S. Recent Advances in the Assembly of High-Nuclearity Lanthanide Clusters. *Coord. Chem. Rev.* **2019**, *378*, 222–236.

[38] Yeung, C.-T.; Yim, K.-H.; Wong, H.-Y.; Pal, R.; Lo, W.-S.; Yan, S.-C.; Yee-Man Wong, M.; Yufit, D.; Smiles, D. E.; McCormick, L. J.; Teat, S. J.; Shuh, D. K.; Wong, W.-T.; Law, G.-L. Chiral Transcription in Self-Assembled Tetrahedral Eu_4L_6 Chiral Cages Displaying Sizable Circularly Polarized Luminescence. *Nat. Commun.* **2017**, *8* (1), 1128.
[39] Knighton, R. C.; Soro, L. K.; Lecointre, A.; Pilet, G.; Fateeva, A.; Pontille, L.; Francés-Soriano, L.; Hildebrandt, N.; Charbonnière, L. J. Upconversion in Molecular Hetero-Nonanuclear Lanthanide Complexes in Solution. *Chem. Commun.* **2021**, *57* (1), 53–56.
[40] Bozoklu, G.; Gateau, C.; Imbert, D.; Pécaut, J.; Robeyns, K.; Filinchuk, Y.; Memon, F.; Muller, G.; Mazzanti, M. Metal-Controlled Diastereoselective Self-Assembly and Circularly Polarized Luminescence of a Chiral Heptanuclear Europium Wheel. *J. Am. Chem. Soc.* **2012**, *134* (20), 8372–8375.
[41] Chen, X.-Y.; Bretonnière, Y.; Pécaut, J.; Imbert, D.; Bünzli, J.-C.; Mazzanti, M. Selective Self-Assembly of Hexameric Homo- and Heteropolymetallic Lanthanide Wheels: Synthesis, Structure, and Photophysical Studies. *Inorg. Chem.* **2007**, *46* (3), 625–637.
[42] Tan, Y. B.; Okayasu, Y.; Katao, S.; Nishikawa, Y.; Asanoma, F.; Yamada, M.; Yuasa, J.; Kawai, T. Visible Circularly Polarized Luminescence of Octanuclear Circular Eu(III) Helicate. *J. Am. Chem. Soc.* **2020**, *142* (41), 17653–17661.
[43] Biswas, S.; Das, S.; Acharya, J.; Kumar, V.; van Leusen, J.; Kögerler, P.; Herrera, J. M.; Colacio, E.; Chandrasekhar, V. Homometallic DyIII Complexes of Varying Nuclearity from 2 to 21: Synthesis, Structure, and Magnetism. *Chem. Eur. J.* **2017**, *23* (21), 5154–5170.
[44] Guettas, D.; Gendron, F.; Fernandez Garcia, G.; Riobé, F.; Roisnel, T.; Maury, O.; Pilet, G.; Cador, O.; Le Guennic, B. Luminescence-Driven Electronic Structure Determination in a Textbook Dimeric DyIII-Based Single-Molecule Magnet. *Chem. Eur. J.* **2020**, *26* (19), 4389–4395.
[45] Rinehart, J. D.; Fang, M.; Evans, W. J.; Long, J. R. Strong Exchange and Magnetic Blocking in N 2 3− -Radical-Bridged Lanthanide Complexes. *Nat. Chem.* **2011**, *3* (7), 538–542.

For Table of Content Only

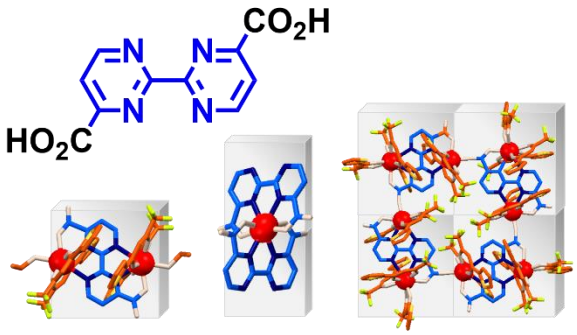

2,2'-bipyrimidine-4,4'-dicarboxylic acid (bpd^{2-}) is a versatile building block for lanthanide coordination, acting both as bridging and chelating ligand. Mononuclear $[Lu(bdp)_2]^-$, $[Lu(bpd)(tta)_2]$-, dinuclear $[Lu_2(bpd)(tta)_4]$ and octonuclear $[Lu_8(bpd)_4(tta)_{18}]^{4-}$ complexes could be obtained in this study.